Astrophys Space Sci (2009) 323: 261–272
DOI 10.1007/s10509-009-0063-1

ORIGINAL ARTICLE

Asymptotic orbits in the $(N+1)$-body ring problem

K.E. Papadakis

Received: 22 April 2009 / Accepted: 19 June 2009 / Published online: 1 July 2009

Abstract In this paper we study the asymptotic solutions of the $(N+1)$-body ring planar problem, N of which are finite and $\nu = N-1$ are moving in circular orbits around their center of masses, while the Nth $+1$ body is infinitesimal. ν of the primaries have equal masses m and the Nth most-massive primary, with $m_0 = \beta m$, is located at the origin of the system. We found the invariant unstable and stable manifolds around hyperbolic Lyapunov periodic orbits, which emanate from the collinear equilibrium points L_1 and L_2. We construct numerically, from the intersection points of the appropriate Poincaré cuts, homoclinic symmetric asymptotic orbits around these Lyapunov periodic orbits. There are families of symmetric simple-periodic orbits which contain as terminal points asymptotic orbits which intersect the x-axis perpendicularly and tend asymptotically to equilibrium points of the problem spiraling into (and out of) these points. All these families, for a fixed value of the mass parameter $\beta = 2$, are found and presented. The eighteen (more geometrically simple) families and the corresponding eighteen terminating homo- and heteroclinic symmetric asymptotic orbits are illustrated. The stability of these families is computed and also presented.

Keywords $(N+1)$-body ring problem · Asymptotic orbits · Homoclinic orbits · Heteroclinic orbits

K.E. Papadakis (✉)
Department of Engineering Sciences, Division of Applied Mathematics and Mechanics, University of Patras, 26504 Patras, Greece
e-mail: k.papadakis@des.upatras.gr

1 Introduction and equations of motion

Poincaré (1957), while studying the so-called Poincaré map associated with an unstable periodic orbit, defined a homoclinic point as a point whose orbit is asymptotic to the hyperbolic fixed point in both directions. Also, Strömgren in 1935 calculated heteroclinic asymptotic orbits connecting the two triangular critical points in the classical restricted three-body problem. After that, many papers have been written about stable and unstable invariant manifolds and homoclinic, heteroclinic, asymptotic orbits associated with an equilibrium point or with a Lyapunov periodic orbit (among others Deprit and Henrard 1965; Conley 1968; McGehee 1969; Llibre and Simó 1980; Llibre et al. 1985; Gómez et al. 1988). The interest in these concepts has been revived recently due to the fact that stable and unstable manifold tubes associated with bounded orbits around the collinear libration points L_1 and L_2, provide a framework for understanding dynamical phenomena such as the conduction particles to and from the smaller primary body and between primaries for separate three-body systems (for details see Koon et al. 1999, 2001b, 2001a; Gómez et al. 2004).

Our goal in this paper is to study the asymptotic solutions around periodic orbits and around the equilibrium points of the planar $(N+1)$-body ring problem. We will calculate the invariant stable and unstable manifolds and the corresponding homoclinic asymptotic orbits around the Lyapunov periodic solutions as well as the homo- and heteroclinic orbits associated with the equilibrium configurations of this problem.

The planar $(N+1)$-body ring problem is a two degrees of freedom problem and describes the motion of an infinitesimal particle attracted by the gravitational field of $\nu+1$ primary bodies $(N = \nu+1)$. We consider a central primary body of mass $m_0 = \beta m$ which is located at the center of

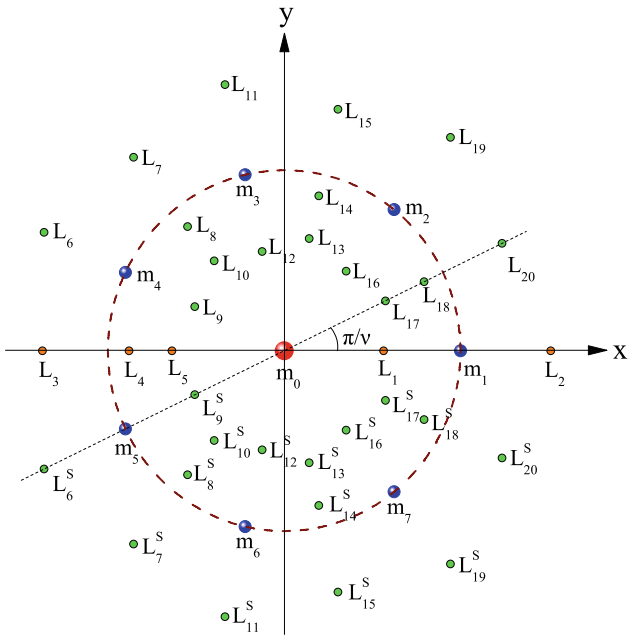

Fig. 1 The positions of the primaries and the distribution of the 35 equilibrium points in the $(8+1)$-body ring problem for $\beta = 2$

a regular of ν-polygon (the origin of the coordinate system; see Fig. 1) and $m_i, i = 1, \ldots, \nu$ peripheral primaries of equal mass m which are located at the vertices of this regular polygon, which is rotating in its own plane about the center with a constant angular velocity.

The equations of motion of the infinitesimal mass, of the $(N+1)$-body ring problem, in the usual dimensionless rectangular rotating coordinate system are written as (Kalvouridis 1999),

$$\begin{aligned} \ddot{x} - 2\dot{y} &= \frac{\partial \Omega}{\partial x} = x - \frac{1}{\Delta}\left(\frac{\beta x}{r_0^3} + \sum_{i=1}^{\nu} \frac{x - x_i}{r_i^3}\right), \\ \ddot{y} + 2\dot{x} &= \frac{\partial \Omega}{\partial y} = y - \frac{1}{\Delta}\left(\frac{\beta y}{r_0^3} + \sum_{i=1}^{\nu} \frac{y - y_i}{r_i^3}\right), \end{aligned} \tag{1}$$

where dots denote time derivatives, while the gravitational potential Ω in synodic coordinates is defined as

$$\Omega = \frac{1}{2}(x^2 + y^2) + \frac{1}{\Delta}\left(\frac{\beta}{r_0} + \sum_{i=1}^{\nu} \frac{1}{r_i}\right), \tag{2}$$

where

$$\begin{aligned} &\Delta = M(\Lambda + \beta M^2), \quad M = 2\sin\theta, \\ &\Lambda = \sin^2\theta \sum_{i=2}^{\nu} \frac{1}{\sin[(i-1)\theta]}, \quad i = 1, \ldots, \nu \end{aligned} \tag{3}$$

and $\theta = \frac{\pi}{\nu}$ is the angle formed between consecutive peripheral primaries. The distances of the particle from the central primary and from each peripheral ones are correspondingly

$$r_0^2 = x^2 + y^2, \quad r_i^2 = (x - x_i)^2 + (y - y_i)^2, \tag{4}$$

while the $\nu = N - 1$ peripheral primary bodies are placed at positions (x_i, y_i):

$$x_i = \frac{1}{M}\cos[2(i-1)\theta], \quad y_i = \frac{1}{M}\sin[2(i-1)\theta]. \tag{5}$$

Here, $\beta = m_0/m$ i.e. is the ratio of the central mass m_0 to one of the other equal primaries, and the unit of length is chosen in such a way that the distance between the primaries is equal to 1.

The energy (Jacobi) integral of this problem is given by the expression

$$\dot{x}^2 + \dot{y}^2 = 2\Omega - C, \tag{6}$$

where C is the Jacobi constant.

2 Linearization around the equilibrium configurations

In the present work we study the $(N+1)$-body ring problem when the number ν of peripheral primaries is $\nu = N - 1 = 7$ and the mass parameter β of the problem is $\beta = m_0/m = 2$.

2.1 Collinear equilibrium points $L_i, i = 1, \ldots, 5$

The linearized equations for infinitesimal motions near the collinear equilibrium points are

$$\dot{\mathbf{x}} = \boldsymbol{A}\mathbf{x}, \quad \mathbf{x} = (x, y, \dot{x}, \dot{y})^T, \tag{7}$$

where $\mathbf{x}$ is the state vector of the ninth particle with respect to the equilibrium points and the time-independent coefficient matrix $\boldsymbol{A}$ is

$$\boldsymbol{A} = \begin{pmatrix} 0 & 0 & 1 & 0 \\ 0 & 0 & 0 & 1 \\ A_{11} & 0 & 0 & 2 \\ 0 & A_{22} & -2 & 0 \end{pmatrix}, \tag{8}$$

where

$$\begin{aligned} A_{11} &= 1 + \frac{1}{\Delta}\left\{\frac{2\beta}{|x_0|^3} + \sum_{i=1}^{7} \frac{2(x_0 - x_i)^2 - y_i^2}{[(x_0 - x_i)^2 + y_i^2]^{5/2}}\right\}, \\ A_{22} &= 1 - \frac{1}{\Delta}\left\{\frac{\beta}{|x_0|^3} + \sum_{i=1}^{7} \frac{(x_0 - x_i)^2 - 2y_i^2}{[(x_0 - x_i)^2 + y_i^2]^{5/2}}\right\}, \end{aligned} \tag{9}$$

and x_0 is the abscissa of the collinear equilibrium point as solution of the equation,

$$x_0 - \frac{1}{\Delta}\left\{\frac{x_0\beta}{|x_0|^3} + \sum_{i=1}^{7} \frac{x_0 - x_i}{[(x_0 - x_i)^2 + y_i^2]^{3/2}}\right\} = 0. \tag{10}$$

The characteristic equation of the linear system (7) is

$$\lambda^4 + (4 - A_{11} - A_{22})\lambda^2 + A_{11}A_{22} = 0. \tag{11}$$

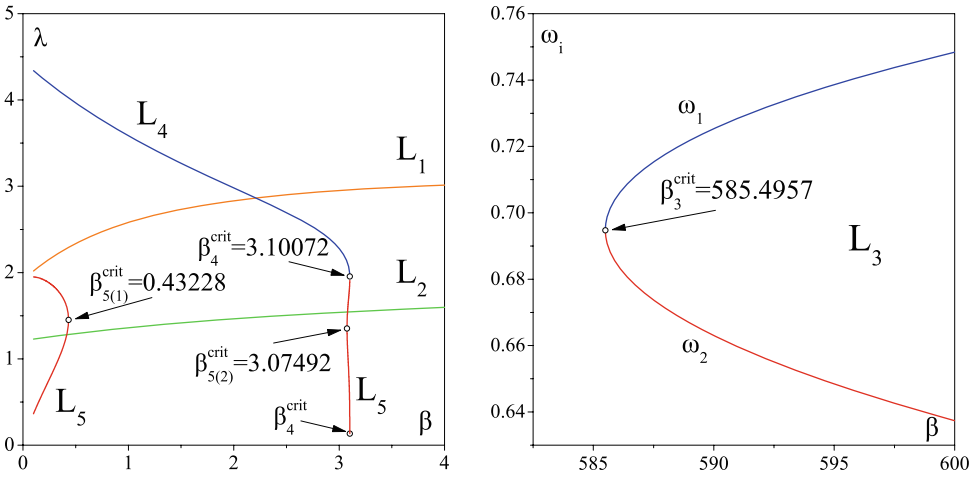

Fig. 2 *Left*: the positive quantity λ at the collinear equilibrium points L_i, $i = 1, 2, 4, 5$ as the mass parameter β varies. *Right*: the eigenfrequencies at the libration point L_3

In the present ring problem, where the number of the peripheral primaries is $\nu = 7$, we have five collinear equilibrium points for $0 < \beta < \beta_4^{\rm crit} = 3.10072$ (the system has 5ν collinear and non-collinear equilibrium points; see Fig. 1). For $\beta = \beta_4^{\rm crit}$ the equilibrium point L_4 coincides with the L_5 and the collinear equilibria are four (4ν equilibria as a whole) and finally for $\beta > \beta_4^{\rm crit}$ the equilibrium points $L_{4,5}$ do not exist (the system now has 3ν collinear and non-collinear equilibrium points).

For the equilibria L_1, L_2 and L_4 the characteristic equation (11) has one real and one imaginary pair of eigenvalues, which have the form $\pm\lambda$ and $\pm i\rho$ where λ and ρ are the positive constants

$$\lambda = \frac{1}{\sqrt{2}}\sqrt{A_{11} + A_{22} - 4 + K},$$
$$\rho = \frac{1}{\sqrt{2}}\sqrt{4 - A_{11} - A_{22} + K}, \tag{12}$$

where

$$K = \sqrt{(A_{11} - 4)^2 - 2(A_{11} + 4)A_{22} + A_{22}^2}. \tag{13}$$

For the collinear equilibrium point L_3 the characteristic equation (11) has, when $0 < \beta < \beta_3^{\rm crit} = 585.4957$, four conjugate complex roots, while when $\beta \geq \beta_3^{\rm crit}$ it has the imaginary roots $\lambda_{1,2} = \pm i\omega_1$ and $\lambda_{3,4} = \pm i\omega_2$ (see Fig. 2, right frame). For the last collinear equilibrium point L_5 (11) has four real roots (when $0 < \beta \leq \beta_{5(1)}^{\rm crit} = 0.43228$), four conjugate complex roots (when $\beta_{5(1)}^{\rm crit} < \beta < \beta_{5(2)}^{\rm crit} = 3.07492$) and four real roots again (when $\beta_{5(2)}^{\rm crit} \leq \beta < \beta_4^{\rm crit}$). For $\beta > \beta_4^{\rm crit}$, as we have already mentioned, the equilibrium points L_4 and L_5 do not exist.

From the above eigenvalues we conclude that, in the present problem, all the collinear equilibrium points are unstable except L_3 where it is stable for $\beta \geq \beta_3^{\rm crit}$ contrary to the classical restricted three-body problem, where all the collinear equilibrium points are unstable for every value of the mass ratio μ.

In the left frame of Fig. 2 we present the positive quantity λ (12) at the collinear equilibrium points $L_{1,2,4,5}$ as the mass parameter of the problem β varies. In the right frame of the same figure, the variation of the eigenfrequencies, or mean motions ω_1, ω_2, at the equilibrium point L_3 are illustrated.

The corresponding eigenvectors of matrix $\boldsymbol{A}$ can be normalized to 1,

$$u_1 = (1, -\sigma, \lambda, -\lambda\sigma)^T, \quad w_1 = (1, -i\tau, i\nu, \nu\tau)^T,$$
$$u_2 = (1, \sigma, -\lambda, -\lambda\sigma)^T, \quad w_2 = (1, i\tau, -i\nu, \nu\tau)^T, \tag{14}$$

where σ and τ are the constants

$$\sigma = \frac{-4 - A_{11} + A_{22} + K}{2\sqrt{2}\sqrt{A_{11} + A_{22} - 4 + K}},$$
$$\tau = \frac{-4 - A_{11} + A_{22} - K}{2\sqrt{2}\sqrt{A_{11} + A_{22} - 4 - K}}. \tag{15}$$

In Fig. 6 we present the zero velocity curves of the $(8 + 1)$-body ring problem for $\beta = 2$ using for Jacobi constant C the values of the energy of the collinear equilibrium points of the problem. For $C = C_{L_5} = 7.27932$ (similarly for $C = C_{L_3} = 6.98058$) zero velocity curve around the equilibrium point L_5 (similarly around L_3) does not exist because the L_5 (respectively the L_3) is a local minimum of the zero velocity surface. In order to plot the zero velocity curve around the equilibrium point L_5 we took, in the third frame of Fig. 6, the Jacobi constant C to be just larger than C_{L_5}. The same we did in the fifth frame where C is just larger than C_{L_3}. The light gray color corresponds to areas where no motion is possible (for details see Kalvouridis 1999).

It is known, in the restricted three-body problem, that from collinear equilibrium points L_i, $i = 1, 2, 3$, emanate the families a (from L_2), b (from L_3) and c (from L_1) (according to the classical nomenclature). For Jacobi constants

C just below of C_{L_i} hyperbolic periodic orbits around each L_i exist, called Lyapunov orbits. Similarly, in the $(8+1)$-body ring problem, emanates the Lyapunov family f_{14} from the collinear equilibrium point L_1 and the family f_{13} from L_2, as we will see in Fig. 3 of next section.

Using the eigenvectors (14) we will find the invariant unstable and stable manifolds around the above hyperbolic Lyapunov periodic orbits which emanate from these equilibria.

2.2 Lagrangian equilibrium points out of x-axis

To study analytically the solutions in the neighborhood of the equilibrium configuration L_i and L_i^S, $i = 6, 7, \ldots, 20$ (see Fig. 1), we can transfer the origin at L_i (L_i^S), and we can linearize the equations of motion as in the previous subsection. But due to the formulation of the problem, the system has symmetry: (a) with respect to the line from the central primary (origin) to any peripheral primary (i.e. the x-axis) and (b) to the line from the central primary to the bisector between two peripheral primaries (see Fig. 1, dotted line). Due to these symmetries all the equilibrium points have to be placed on those lines. So on the x-axis, for $\beta = 2$, we have the equilibrium points L_i, $i = 1, \ldots, 5$, while on the bisector line between the primaries m_1 and m_2 we have the collinear, with respect to this line, equilibria $L_{17,18,20}$ and $L_{6,9}^S$; then on the next bisector between m_2 and m_3 lie the $L_{13,14,15}$ and $L_{11,12}^S$ and so on (see Fig. 1).

The five groups of equilibrium points which exhibit the same behavior, with respect to linear stability, are

(a) $L_1, L_9, L_9^S, L_{12}, L_{12}^S, L_{16}, L_{16}^S$,
(b) $L_2, L_6, L_6^S, L_{11}, L_{11}^S, L_{19}, L_{19}^S$,
(c) $L_3, L_7, L_7^S, L_{15}, L_{15}^S, L_{20}, L_{20}^S$,
(d) $L_4, L_8, L_8^S, L_{14}, L_{14}^S, L_{18}, L_{18}^S$,
(e) $L_5, L_{10}, L_{10}^S, L_{13}, L_{13}^S, L_{17}, L_{17}^S$.

In the previous subsection we studied the stability of the collinear equilibrium points L_i, $i = 1, \ldots, 5$ and due to the symmetries we have, actually, already studied the stability for all the equilibrium points out of the x-axis. So, all the equilibrium points of this problem are unstable, for every value of the mass parameter β for which they exist, except the L_3, L_7, L_7^S, L_{15}, L_{15}^S, L_{20} and L_{20}^S, which are stable for $\beta \geq \beta_3^{\text{crit}}$.

In that last case we have a solution with "short" and "long" period terms corresponding to large and small values of the eigenfrequencies ω_1, ω_2 (for details see p. 258 of Szebehely 1967).

3 Asymptotic orbits around equilibrium points

In this section we present all the families of simple symmetric periodic orbits (i.e. having only two both perpendicular, intersections with the x-axis) for $\beta = 2$, where their termination members are asymptotic orbits to equilibrium points of the problem spiraling into (and out of) these points. We found decades of such families and we present the eighteen more geometrically simple of them, named f_i, $i = 1, \ldots, 18$, as well as the asymptotic orbits which are associated to these families.

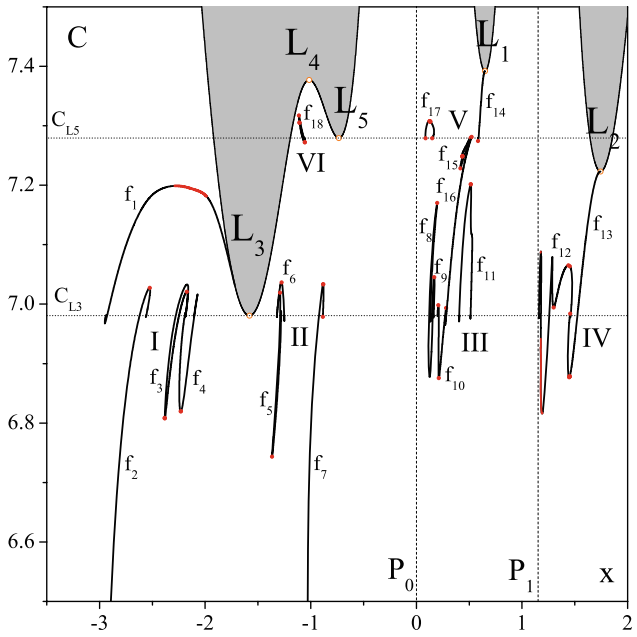

Fig. 3 Families of simple symmetric periodic orbits where their termination orbits are asymptotic, in the $(8+1)$-body ring problem for $\beta = 2$

In Fig. 3 we present the network of these eighteen families while the heavy red lines indicate their horizontal stable arcs. The small circles are the positions of the five collinear equilibrium points and the gray color corresponds to areas where no motion is possible.

All the characteristic curves of these families, as we see in this figure, spiral from one or both sides around the points, in the (x_0, C) plane, where they have $C = C_{L_3}$ or $C = C_{L_5}$. These are the natural termination points near areas I–VI, which are presented in Fig. 3. Details of the areas of these points are illustrated in the six frames of Fig. 4. Typical terminating asymptotic orbits of these eighteen families are plotted in Fig. 5, while data of some of these orbits are presented in Table 1.

Two of these families have as terminating members homoclinic asymptotic orbits at the collinear equilibrium points L_3 and L_5. Specifically, family f_4 from one side has as a termination member a homoclinic asymptotic orbit at the collinear equilibrium point L_3 and from the other side ends with a heteroclinic asymptotic orbit at the equilibrium points L_7 and L_7^S. Contrarily, family f_{15} starts and ends with a homoclinic asymptotic orbit at the collinear equilibrium point L_5.

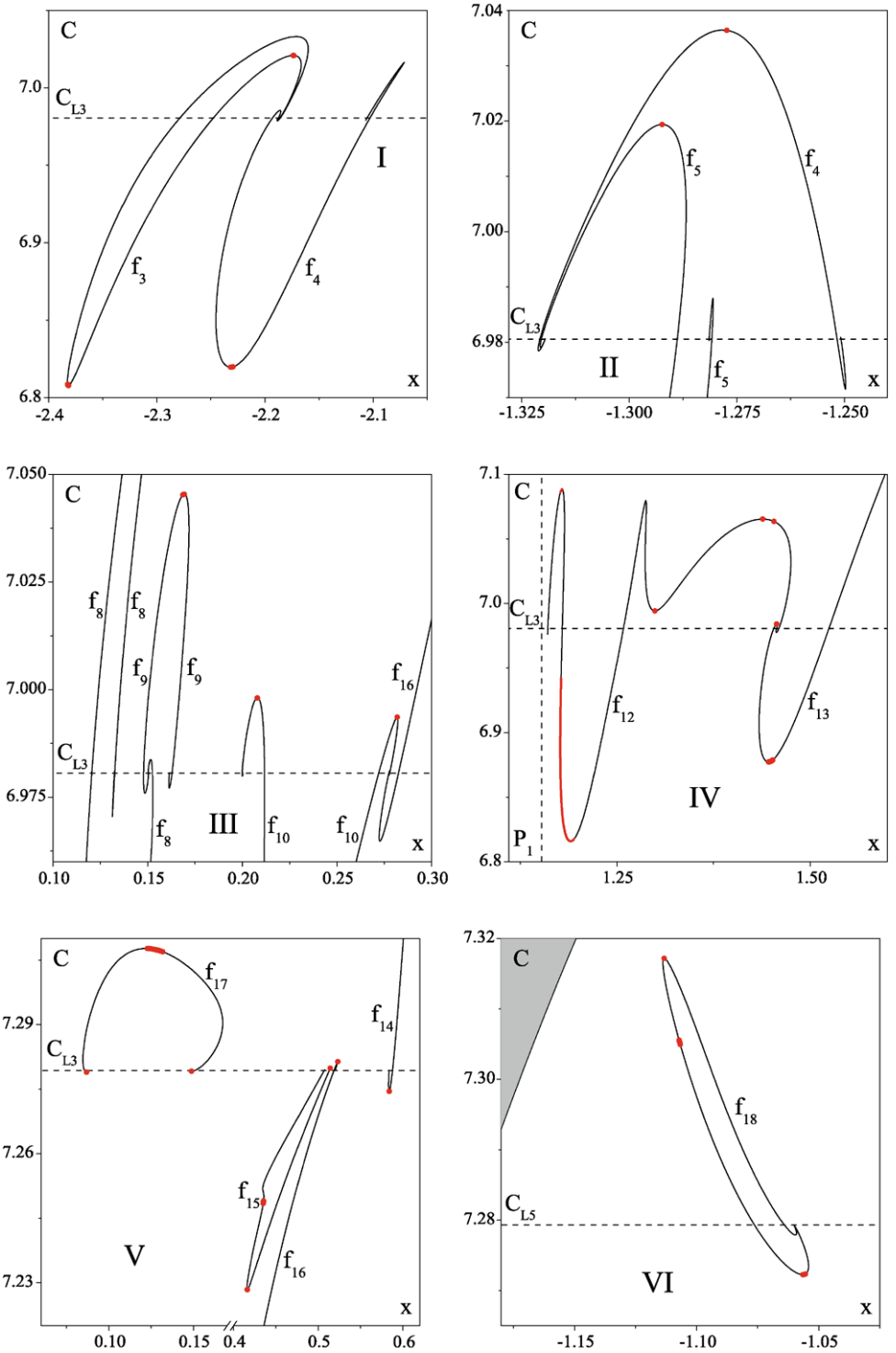

Fig. 4 Zooming in around the areas I, II, III, IV, V and VI of Fig. 3

Two other families emanate from equilibrium points, namely, the family f_{14} emanates from the collinear equilibrium point L_1 and ends with a heteroclinic asymptotic orbit at the equilibrium points L_{17} and L_{17}^S, while family f_{13} emanates from L_2 and ends with a heteroclinic asymptotic orbit at L_{20} and L_{20}^S.

As well, family f_2 from one side starts with a heteroclinic asymptotic orbit at L_{15} and L_{15}^S, while the other side continues out of the frame of Fig. 3 for smaller values of the Jacobi constant C. Similarly, family f_7 from one side starts with a heteroclinic asymptotic orbit at L_7 and L_7^S while the other side continues for smaller C.

Table 1 Data of some asymptotic orbits illustrated in Fig. 5

Family	x_0	$x_{T/2}$	$\dot{y}_{T/2}$	C	$T/2$	Stability	Orbit
f_1	−2.93997091	1.99930414	−0.70829296	6.98057737	19.45426383	U	Heteroclinic at L_{20}, L_{20}^S
f_2	−2.55991161	0.78051638	−0.78805488	6.98057953	16.39918836	U	Heteroclinic at L_{15}, L_{15}^S
f_4	−2.10553344	−1.58083557	0.00000007	6.98057667	19.33053956	U	Homoclinic at L_3
f_5	−1.31961525	−0.41723618	−1.03537365	6.98058296	16.80818734	U	Heteroclinic at L_7, L_7^S
f_{13}	1.45658367	1.99930414	−0.70829350	6.98057663	17.41913222	U	Heteroclinic at L_{20}, L_{20}^S
f_{14}	0.58387238	0.71877558	−0.40985792	7.27931806	11.02592491	U	Heteroclinic at L_{17}, L_{17}^S
f_{15}	0.51279332	−0.73403890	0.00000004	7.27931806	13.89829146	U	Homoclinic at L_5
f_{16}	0.52001479	−0.65721568	−0.16743922	7.27931809	14.91087210	U	Heteroclinic at L_{13}, L_{13}^S
f_{17}	0.08775510	−0.98493340	−0.30832720	7.27931818	10.67219854	U	Heteroclinic at L_{10}, L_{10}^S

Table 2 Terminating heteroclinic orbits

Family	One side of the family	Other side
f_3	at L_7, L_7^S	at L_7, L_7^S
f_5	at L_7, L_7^S	at L_{15}, L_{15}^S
f_6	at L_7, L_7^S	at L_{20}, L_{20}^S
f_8	at L_7, L_7^S	at L_{15}, L_{15}^S
f_9	at L_{15}, L_{15}^S	at L_{15}, L_{15}^S
f_{10}	at L_7, L_7^S	at L_7, L_7^S
f_{11}	at L_{15}, L_{15}^S	at L_{15}, L_{15}^S
f_{12}	at L_{15}, L_{15}^S	at L_{20}, L_{20}^S
f_{16}	at L_7, L_7^S	at L_{13}, L_{13}^S
f_{17}	at L_{10}, L_{10}^S	at L_{10}, L_{10}^S
f_{18}	at L_{10}, L_{10}^S	at L_{10}, L_{10}^S

The first family f_1 starts with a heteroclinic asymptotic orbit at L_{20} and L_{20}^S and ends on the zero velocity curve.

All the rest of the families have as terminating members heteroclinic orbits at various equilibrium points out of the x-axis, as presented in Table 2.

We note here that a homoclinic orbit related to an equilibrium point L or to a periodic orbit P is an orbit that tends to L (or to P) for $t \to \pm\infty$, while a heteroclinic orbit "joins" two equilibrium points or two periodic orbits.

The majority of the symmetric periodic orbits of the families we found is unstable, but from Figs. 3 and 4 we can see that small arcs of stable periodic orbits exist (heavy red lines). The termination of these eighteen families have a characteristic behavior. As the period tends to infinity, the energy of the orbits oscillates in a small shrinking interval around the energy of the asymptotic orbit which is the energy of the equilibrium point ($L_{3(5)}$).

At each change in the sign of the derivative of the energy, the stability of the orbit changes. This type of termination has been called a 'blue sky catastrophe' at first by Abraham (1975) and later by Devaney (1977), who in his paper writes: Let X_τ be a one-parameter family of smooth vector fields depending continuously on a real parameter τ. Suppose that for $\tau < \tau_0$, X_τ has a closed orbit γ_τ and that the γ_τ also depend continuously on τ. We say that X_{τ_0} admits a blue sky catastrophe along γ_τ if the periods of the γ_τ tend to infinity as τ approaches τ_0, i.e. the closed orbits disappear into the "blue sky".

4 Asymptotic orbits around Lyapunov periodic orbits

The contours of the surface (6) for zero velocity provide the zero velocity curves of the $(8+1)$-body ring problem. In Fig. 6 we present these zero velocity curves for $\beta = 2$ and for values of the Jacobi constant C exact or very close to the values of the five collinear equilibrium points. Especially, in the first, second and fourth frame we plot the zero velocity curves for $C = C_{L_1}$, $C = C_{L_4}$ and $C = C_{L_2}$, respectively. In the third and fifth frame we illustrate the zero velocity curves for C just bigger than C_{L_5} and C_{L_3} respectively, in order to create zero velocity curves around the equilibrium points L_5 and L_3. For $C = C_{L_5}$ and $C = C_{L_3}$ the small islands around L_5 and L_3 do not exist. The zero velocity curves in Fig. 6 are classified from the bigger (first frame) to smaller (last one) value of C. The red point is the central primary, the blue ones the peripheral primaries and the green points are the equilibrium points of the problem. The light gray color corresponds to areas where no motion is possible.

For values of the Jacobi constant C greater than or equal to C_{L_1}, the infinitesimal ninth body is free to move only in isolated regions where the central body or one peripheral primary exists (first frame of Fig. 6). But for C just less than C_{L_1} a "neck" around L_1 (and of course around L_9, L_{12}, etc.; see group (a) in Sect. 2.2) is created and now the small body can move from the central primary body to the peripherals and vice versa. This region, as the Hill's region (keeping the same terminology as in the restricted three-body problem), corresponding to such values of the Jacobi constant, contains "necks" around the equilibrium points.

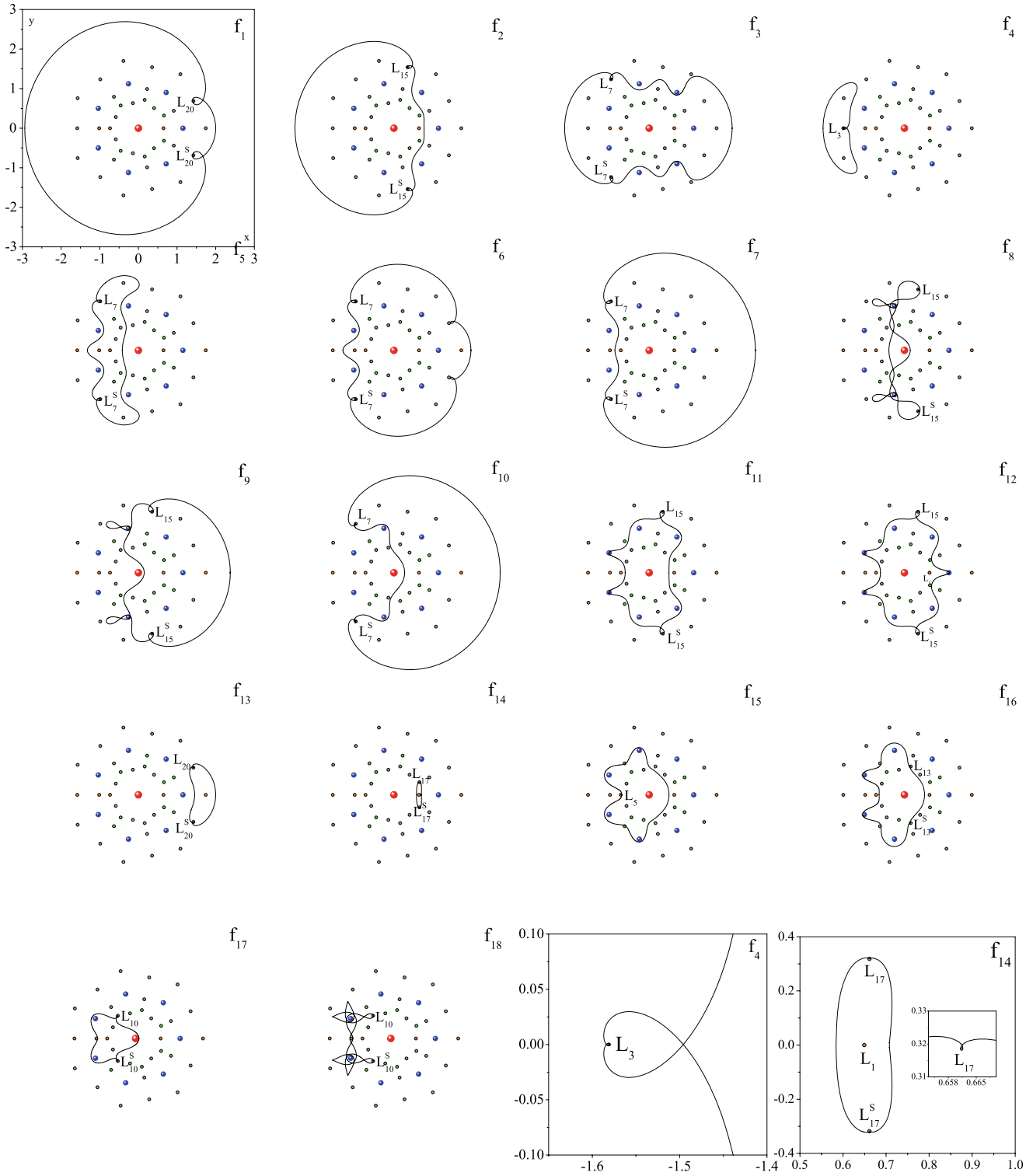

Fig. 5 Asymptotic orbits from the 18 families plotted in Fig. 3. Last two frames: details of orbits from f_4 and f_{14} families correspondingly. In each frame the equilibrium points around which these asymptotic orbits exist, are marked. Data of some of these orbits are presented in Table 1. The *red point* is the central primary, the *blue* ones the peripheral primaries and the *green* ones the equilibrium points of the problem

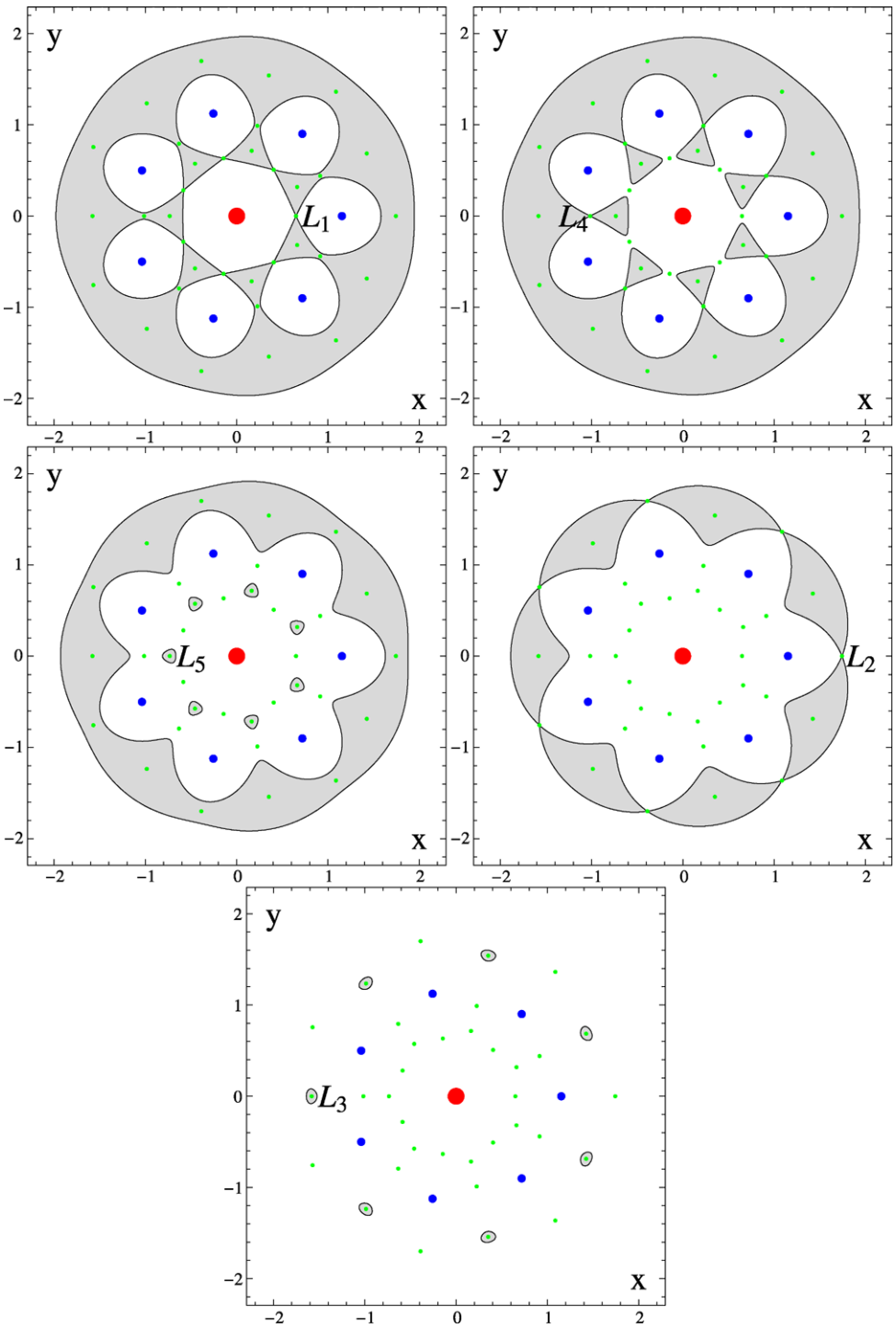

Fig. 6 Zero velocity curves of the $(8+1)$-body ring problem for $\beta = 2$. The Jacobi constant C is, from the first to fifth frame (from the bigger to smaller values of C), $C_{L_1} = 7.3919$, $C_{L_4} = 7.37704$, $C_{L_5} \simeq 7.3$, $C_{L_2} = 7.22324$, $C_{L_3} \simeq 6.99$, respectively. The *red point* is the central primary, the *blue* ones are the peripheral primaries and the *green* ones the equilibrium points of the problem. The *light gray color* corresponds to areas where no motion is possible

As we saw in the previous section, family f_{14} of symmetric periodic orbits which emanate from the equilibrium point L_1 contains hyperbolic Lyapunov orbits for $C < C_{L_1}$.

In this section we have done a systematic numerical computation of the invariant unstable $W^{\mathrm{u}}_{\mathrm{L_{1p.o.}}}$ manifolds associated with these Lyapunov periodic orbits and the corresponding homoclinic asymptotic orbits which exist around them.

For values of the Jacobi constant C greater than or equal to C_{L_2}, the infinitesimal body is free to move only in the white internal region of the fourth frame of Fig. 6 and cannot move out of this. When C is just less than C_{L_2} a "neck" around L_2 (and of course around L_6, L_{11} etc.; see group (b) in Sect. 2.2) is created and now the small body can move out of the bodies' region and around them. Family f_{14} of symmetric periodic orbits emanates from the equilibrium point

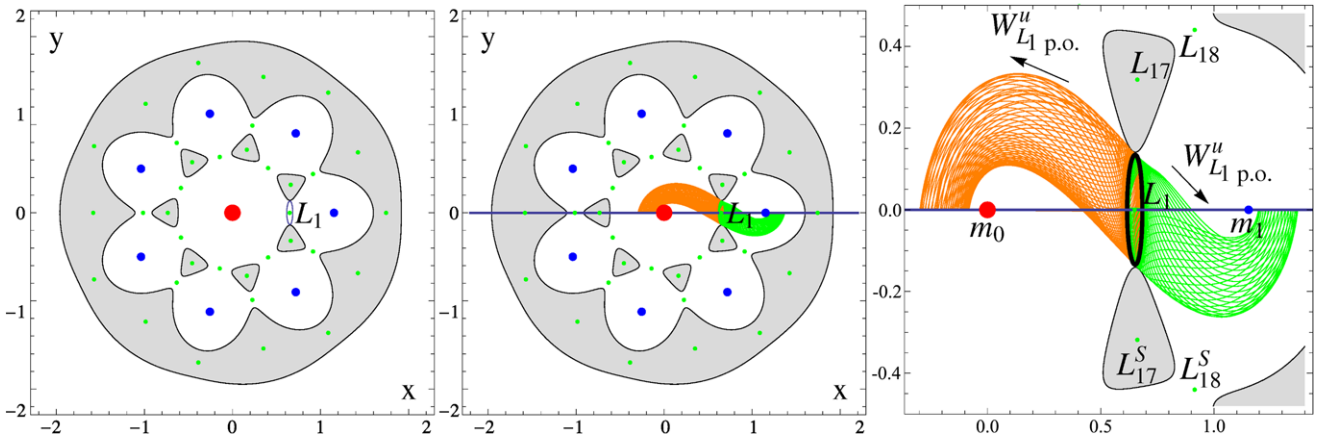

Fig. 7 *Left*: zero velocity curves and a Lyapunov periodic orbit around the equilibrium point L_1 for $C = 7.350092$. *Middle*: the unstable manifolds $W^{\text{u}}_{\text{L}_1\text{p.o.}}$ of this Lyapunov periodic orbit. *Right*: details of the unstable manifolds

L_1 and contains hyperbolic Lyapunov orbits for $C < C_{L_2}$. And in this case we found homoclinic asymptotic orbits around these Lyapunov periodic orbits.

We note that if we know the unstable manifold of a Lyapunov orbit, then the corresponding stable manifold is obtained using the symmetric property of the equations of the problem. The equations of motion of the $(N+1)$-body ring problem, as in the classical three-body one, have the property that if $x = x(t)$, $y = y(t)$ is a solution, then $x = x(-t)$, $y = -y(-t)$ is also a solution. This symmetry follows from inspection of the terms occurring in the differential equations (1), where if we substitute $x \to x$, $y \to -y$, $\dot{x} \to -\dot{x}$, $\dot{y} \to \dot{y}$, $\ddot{x} \to \ddot{x}$ and $\ddot{y} \to -\ddot{y}$, the equations remain unchangeable, a fact that verifies the preceding statement.

Using the analysis of Deprit and Henrard (1969), or the analysis of Llibre et al. (1985), or the purely numerical method presented by Simó and Stuchi (2000), we can determine the invariant unstable manifold $W^{\text{u}}_{\text{L}_i\text{p.o.}}$ emerging from each unstable Lyapunov orbit close to any of the collinear equilibrium points L_1 and L_2. It is known (Conley 1968) that unstable (and stable $W^{\text{s}}_{\text{p.o.}}$) manifolds of these Lyapunov orbits are two dimensional, locally diffeomorphic to cylinders (e.g. Fig. 7, third frame). In this way we compute the surface of section of the invariant manifold with the plane $y = 0$ one or two or more times, and obtain a closed curve which is diffeomorphic to a circle (e.g. first frame of Fig. 8). We call this intersection the (first or second, etc.) "cut" of $W^{\text{u}}_{\text{L}_i\text{p.o.}}$ with the appropriate plane.

In the first frame of Fig. 7 we present the zero velocity curves of the problem for $C = 7.350092$, i.e. just a smaller value than the energy of the collinear equilibrium point $C_{L_1} = 7.3919$ where a small "neck" around L_1 has been created. A hyperbolic Lyapunov periodic orbit around the equilibrium point is also plotted. This Lyapunov periodic orbit belongs to the family f_{14}, which emanates from the collinear equilibrium point L_1 as we have already mentioned in the previous section.

In the next frame in the same figure we illustrate the position space projection of the unstable manifold $W^{\text{u}}_{\text{L}_1\text{p.o.}}$ (orange-green tube) until the first intersection with the Poincaré section at $y = 0$. Details of this unstable manifold are presented in the third frame of the same figure.

Then we calculated the first Poincaré cut of the left (orange) unstable manifold $W^{\text{u}}_{\text{L}_1\text{p.o.}}$ with the plane $y = 0$ for the same value of the Jacobi constant and we plot it (line C_3) in the first frame of Fig. 8. This line has no intersection with the line $\dot{x} = 0$. For smaller values of C than C_3 the first Poincaré cuts have been shrunk (lines C_2 and C_1), while for larger values of C we have the lines C_4 and C_5. So, for $C = 7.30542191$ the first Poincaré cut has two intersections with the $\dot{x} = 0$, named A and B and we will call them homoclinic points, since they are initial conditions for homoclinic asymptotic orbits around the Lyapunov periodic orbit with the same energy.

Similarly, we plot, in the second frame of Fig. 8, the first Poincaré cuts of the right (green) unstable manifold $W^{\text{u}}_{\text{L}_1\text{p.o.}}$ with the plane $y = 0$ for the same value of the Jacobi constant C_i, $i = 1, \ldots, 5$ as in the previous frame. We observe that for $C = C_4$ and $C = C_5$ we have homoclinic points. We choose only the homoclinic points D and E for $C = C_5 = 7.30542191$ in order to have homoclinic points with the same energy as in the left Poincaré cut projection.

Using the initial conditions of the homoclinic points A, B, D and E and the common value of the Jacobi constant C_5 (i.e. $\mathbf{x_0} = (x_0, 0, 0, \dot{y}_0(C_5))$), we produce the homoclinic trajectories which are presented in the third frame of Fig. 8.

So far, we have studied the asymptotic orbits, around the Lyapunov periodic orbit, in the case where the energy constant has the value $C = 7.305422$ and the region where the

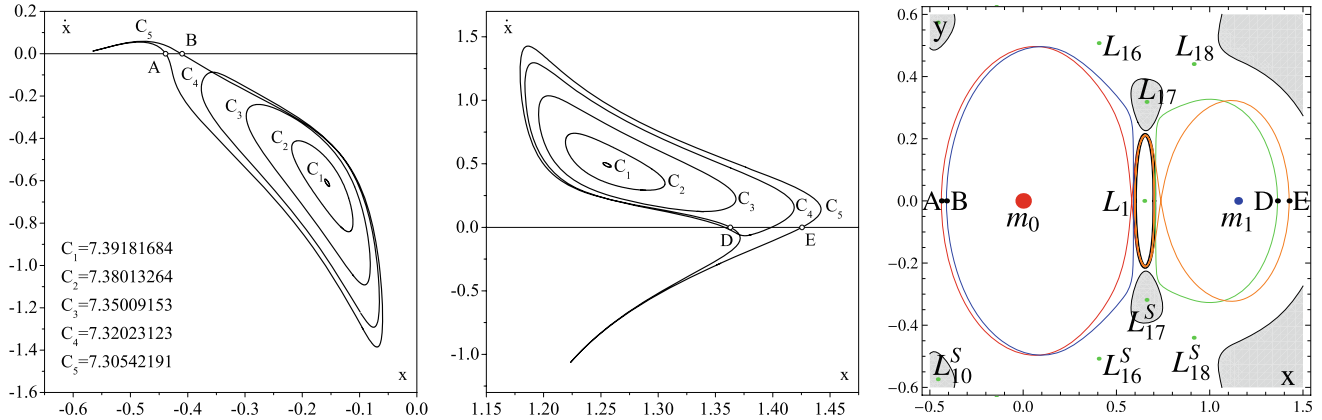

Fig. 8 *Left*: the first Poincaré cuts of the left unstable invariant manifold $W^{u}_{L_1 p.o.}$ with the plane $y = 0$ around the equilibrium point L_1 for various values of C. *Middle*: the first Poincaré cuts of the right unstable manifolds. *Right*: The Lyapunov periodic orbit around the equilibrium point L_1 with $C = 7.305422$ (*black*) and the corresponding homoclinic orbits with initial conditions of the homoclinic points A (*red*), B (*blue*), D (*green*) and E (*orange*)

infinitesimal body can move free, is closed, and fourteen (two of them are collinear) of the equilibrium points of the $(8+1)$-body ring problem are out of it. Now we decrease the energy and we take $C = 7.102558$ (a value just below the energy of L_2) where the closed region opens and new "necks" close to equilibrium points L_2, L_{19} etc., exist. In that case, and always for $\beta = 2$, the unstable invariant manifolds of the Lyapunov periodic orbit with the same C around the collinear equilibrium point L_2 are calculated. The Lyapunov periodic orbit in this case belongs to family f_{13}, which emanates from the collinear equilibrium point L_2.

Similarly as earlier we compute the appropriate cuts with the plane $y = 0$ in order to find the intersections with the $\dot{x}$-axis (homoclinic intersections). In Fig. 9 (first frame) the first Poincaré cuts of the left unstable manifold of the Lyapunov periodic orbit around L_2 i.e. $W^{u}_{L_{2p.o.}}$ for various values of the Jacobi constant C, are presented. None of them, and for any other values of C of this family, intersects the $\dot{x}$-axis. But if we plot the first Poincaré cuts of the right unstable manifold $W^{u}_{L_{2p.o.}}$, then we observe, in the next three frames of the same Fig. 9, that for $C = C_{4,5,6}$ many homoclinic points exist. We choose only the points F and G from the Poincaré cut $C_4 = 7.102558$ and we calculated the corresponding homoclinic asymptotic orbits around the hyperbolic Lyapunov periodic orbit with the same energy and we present them in the fifth frame of Fig. 9. Details of the area close to collinear equilibrium point L_2 are present in the last frame of the same figure.

5 Conclusions

In this paper, a study of the asymptotic orbits around the equilibrium points and around hyperbolic Lyapunov symmetric periodic orbits of the $(N + 1)$-body ring problem when the mass parameter is $\beta = 2$ and $N = \nu + 1 = 8$ has been done.

We found all the families of symmetric simple-periodic orbits of the problem which contain as terminal points homoclinic or heteroclinic asymptotic orbits which intersect the x-axis perpendicularly and tend asymptotically to equilibrium points of the problem spiraling into (and out of) these points. Eighteen of them, the simplest ones, are plotted in detail. The horizontal isoenergetic stability of these families is calculated. Eighteen typical homo- and heteroclinic asymptotic orbits, one of each family, are illustrated.

We also found the unstable invariant manifold of hyperbolic Lyapunov periodic orbits around the collinear equilibrium points L_1 and L_2. The first Poincaré cuts of the unstable manifolds on the appropriate plane $y = 0$, for various values of the Jacobi constant, are calculated and presented. We determined homoclinic points and using these points as initial conditions, we found homoclinic asymptotic orbits around the Lyapunov periodic orbits with the same energy.

From the obtained results some general remarks are in order.

- We found the critical values of the mass parameter β where they split the kind of the eigenvalues of the linearization system around the collinear equilibrium configurations as the mass parameter β of the problem ($\nu = 7$) varies.
- In the present problem, all the collinear equilibrium points are unstable except L_3, which is stable for $\beta \geq \beta_3^{\text{crit}} = 585.4957$ on contrary to the classical restricted three-body problem, where all the collinear equilibrium points are unstable for every value of the mass ratio μ.
- There are decades of families of simple symmetric periodic orbits (i.e. having only two both perpendicular, intersections with the x-axis). Many of them have as termi-

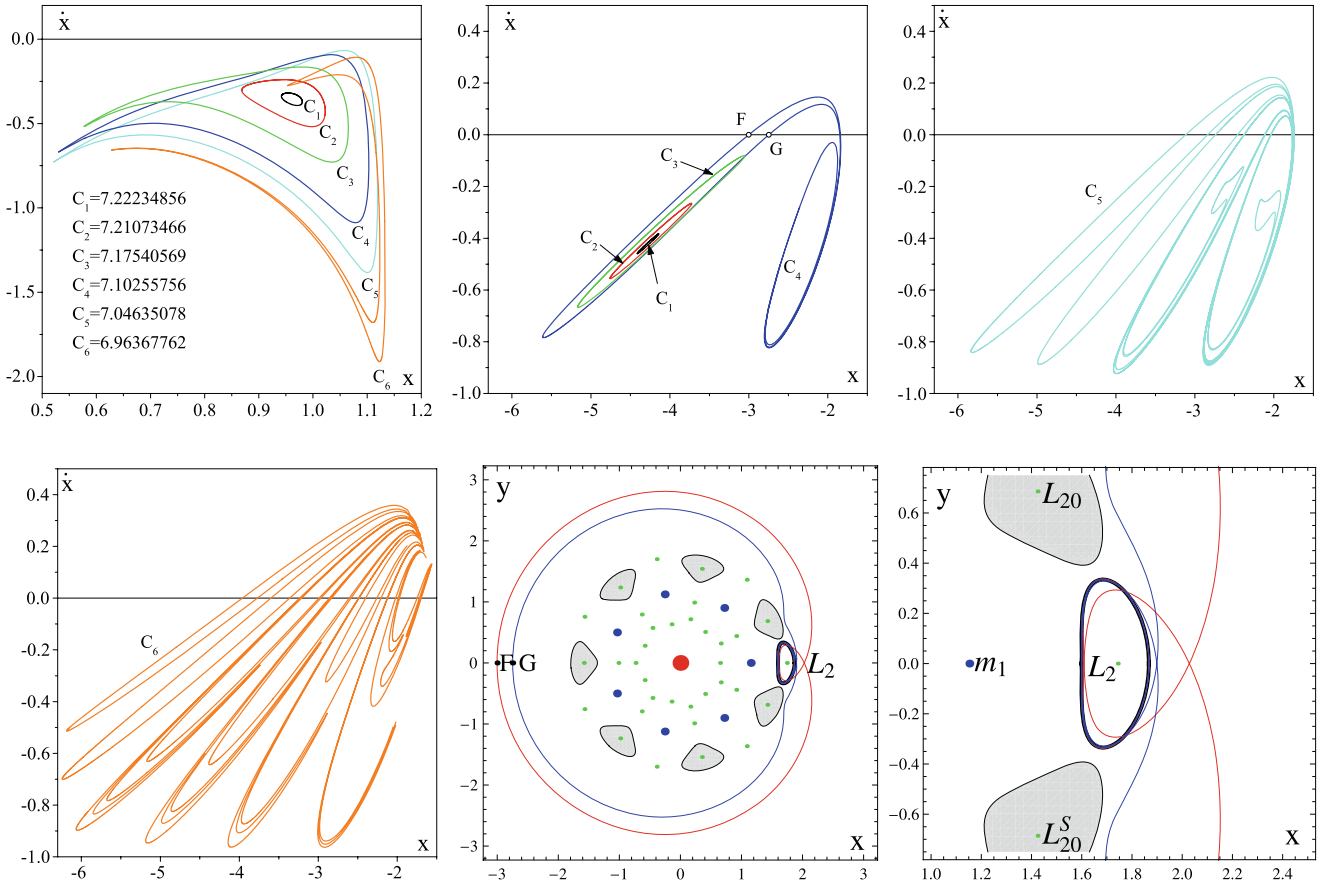

Fig. 9 *Up left*: the first Poincaré cuts of the left unstable invariant manifold $W^{u}_{L_1 p.o.}$ with the plane $y = 0$ around the equilibrium point L_2 for various values of C. *Up middle*: the first Poincaré cuts of the right unstable manifolds for C_1, C_2, C_3 and C_4. *Up left*: the first Poincaré cuts of the right unstable manifolds for C_5. *Down right*: the first Poincaré cuts of the right unstable manifolds for C_6. *Down middle*: the Lyapunov periodic orbit around the equilibrium point L_2 with $C = 7.102558$ (*black*) and the corresponding homoclinic orbits with initial conditions of the homoclinic points F (*red*) and G (*blue*). *Down right*: details close to L_2

nation orbits asymptotic ones at equilibrium points of the problem. From the eighteen families which we study in detail, we conclude to the following.

- Only two families have as members homoclinic asymptotic orbits.
- Sixteen families have heteroclinic asymptotic terminating orbits.
- Eleven families have in both edges as termination members heteroclinic asymptotic orbits.
- There is one family (namely f_{16}) which, from one side, has as terminal member a heteroclinic asymptotic orbit for $C = C_{L_3}$, while from the other side it has as terminal member a heteroclinic asymptotic orbit for $C = C_{L_5}$.
- In the majority of cases, the symmetric periodic orbits of the families we found are unstable but all the families have limited segments of their characteristic curves for which the orbits are stable.
- There are homoclinic asymptotic orbits at the Lyapunov periodic orbits in the interior region (around the central primary body m_0 or the m_1) as well as in the exterior region (around all the eight primary bodies).

References

Abraham, R.: Fifty problems in dynamical systems. In: Dynamical Systems—Warwick, 1974. Lecture Notes, vol. 468. Springer, Berlin (1975)

Conley, C.: SIAM J. Appl. Math. **16**, 732 (1968)

Deprit, A., Henrard, J.: Astron. J. **70**, 271 (1965)

Deprit, A., Henrard, J.: Astron. J. **74**, 308 (1969)

Devaney, R.: Ind. Univ. Math. **26**, 247 (1977)

Gómez, G., Llibre, J., Masdemont, J.: Celest. Mech. **44**, 239 (1988)

Gómez, G., Koon, W.S., Lo, M.W., Marsden, J.E., Masdemont, J., Ross, S.D.: Nonlinearity **17**, 1571 (2004)

Kalvouridis, T.J.: Astrophys. Space Sci. **260**, 309 (1999)

Koon, W.S., Lo, M.W., Marsden, J.E., Ross, S.D.: In: AAS/AIAA Astrodynamics Specialist Conf., Girdwood, Alaska, 1999, paper 99-451. AAS, Washington (1999)

Koon, W.S., Lo, M.W., Marsden, J.E., Ross, S.D.: Celest. Mech. Dyn. Astron. **81**, 27 (2001a)
Koon, W.S., Lo, M.W., Marsden, J.E., Ross, S.D.: Celest. Mech. Dyn. Astron. **81**, 63 (2001b)
Llibre, J., Simó, C.: J. Differ. Equ. **37**, 444 (1980)
Llibre, J., Martínez, R., Simó, C.: J. Differ. Equ. **58**, 104 (1985)
McGehee, R.P.: PhD Thesis, University of Wisconsin (1969)
Poincaré, H.: Le Méthodes Nonvelles de la Mécanique Céleste. Dover, New York (1957)
Simó, C., Stuchi, T.J.: Physica D **140**, 1 (2000)
Szebehely, V.: Theory of Orbits. Academic Press, New York (1967)